

# Pyrolysis of Poly(ferrocenylsilanes): Synthesis and Characterization of Ferromagnetic Transition Metal-Containing Ceramics and Molecular Depolymerization Products

Ruth Petersen,<sup>†</sup> Daniel A. Foucher,<sup>†</sup> Ben-Zhong Tang,<sup>†</sup> Alan Lough,<sup>†</sup>  
Nandyala P. Raju,<sup>‡</sup> John E. Greedan,<sup>‡</sup> and Ian Manners<sup>\*,†</sup>

Department of Chemistry, University of Toronto, 80 St. George St., Toronto M5S 1A1,  
Ontario, Canada, and the Institute for Materials Research, McMaster University,  
Hamilton L8S 4M1, Ontario, Canada

Received February 15, 1995. Revised Manuscript Received August 10, 1995<sup>⊗</sup>

Thermogravimetric analysis (TGA) of a series of high molecular weight poly(ferrocenylsilanes)  $[\text{Fe}(\eta\text{-C}_5\text{H}_4)_2(\text{SiRR}')_n]$  **2a–d** (**a**: R = R' = Me; **b**: R = R' = Ph; **c**: R = Me, R' = H; **d**: R = Me, R' = vinyl) indicated that these materials are thermally stable to ca. 300–350 °C under dinitrogen (heating rate 10 °C/min) and at more elevated temperatures yield the ceramic products **3a–d**. Ceramic yields by TGA were in the range of 18% (for **2b**) to 66% (for **2d**) at 600 °C and in the range of 17% (**2b**) to 45% (**2c**, **2d**) at 1000 °C. Pyrolysis of a 1:1 blend of the polymers **2c** and **2d** afforded the ceramic **3e** in 62% yield at 600 °C and the highest ceramic yield by TGA at 1000 °C (56%). Controlled pyrolysis experiments in a tube furnace under N<sub>2</sub> permitted the isolation of the black, lustrous ceramics **3a–e** together with several molecular depolymerization products. The ceramics **3a** (formed at 600 and 1000 °C) and **3b** and **3e** (formed at 600 °C) were characterized by scanning electron microscopy (SEM) with energy-dispersive X-ray microanalysis (EDX) and back-scattered electron imaging (BEI). These techniques indicated that these materials were iron silicon carbides. The ceramic **3a** formed at 600 °C was found to be amorphous, whereas the corresponding ceramic formed at 1000 °C was shown to contain  $\alpha$ -Fe crystallites by powder X-ray diffraction (XRD). Mössbauer and magnetization measurements carried out on the ceramics **3a**, **3b**, and **3e** indicated that the materials were soft ferromagnets. Identification of several volatile molecular byproducts produced during pyrolysis provided evidence for the operation of unusual decomposition/depolymerization pathways. The unsymmetrical dimer  $\text{Fe}(\eta\text{-C}_5\text{H}_4)_2(\mu\text{-SiMe}_2)_2(\eta\text{-C}_5\text{H}_3)\text{Fe}(\eta\text{-C}_5\text{H}_5)$  (**4a**) was formed during the pyrolysis of **2a**, and this species was characterized by single-crystal X-ray diffraction. Cyclic voltammetry studies of **4a** in CH<sub>2</sub>Cl<sub>2</sub> showed that this species undergoes two reversible and sequential one-electron oxidations (separation  $\Delta E_{1/2} = 0.26$  V) consistent with redox coupling between the iron centers. Triphenylsilylferrocene,  $\text{Fe}(\eta\text{-C}_5\text{H}_5)(\eta\text{-C}_5\text{H}_4\text{SiPh}_3)$ , was isolated as one of the volatile pyrolysis products derived from **2b**. Crystals of **4a** are monoclinic, space group  $P2_1/n$ , with  $a = 9.3842(2)$  Å,  $b = 15.455(2)$  Å,  $c = 15.6630(12)$  Å;  $\beta = 91.092(6)^\circ$ ;  $Z = 4$ ;  $V = 2271.2(11)$  Å<sup>3</sup>.

## Introduction

Polymers are attracting considerable attention as pyrolytic precursors to ceramic fibers and composite materials due to their unique processing advantages.<sup>1–3</sup> To date, most work in this area has focused on the formation of structural ceramics containing main-group elements, for example, SiC, Si<sub>3</sub>N<sub>4</sub>, B<sub>4</sub>C, and BN, which possess useful physical properties such as tensile strength and high thermal stability.<sup>4–9</sup> Transition-metal-containing solid-state materials are also desirable ceramic

products as they can possess interesting electrical and magnetic properties in addition to useful mechanical characteristics. However, preceramic polymer routes to metal-containing ceramics are much less explored and most approaches to such materials have involved chemical modification of preformed preceramic polymers. Recent strategies have included the derivatization of liquid poly(methylsilanes) by dehydrogenative coupling using  $\text{MMe}_2(\eta\text{-C}_5\text{H}_5)_2$  (M = Ti, Zr, or Hf) which yields SiC/MC composites after pyrolysis.<sup>10,11</sup> Other approaches have involved the pyrolysis of poly[(silyl)acetylenes] or other silicon-containing polymers in the presence of transition-metal powders or oxides to yield

<sup>†</sup> University of Toronto.

<sup>‡</sup> McMaster University.

<sup>⊗</sup> Abstract published in *Advance ACS Abstracts*, September 15, 1995.

(1) Aldinger, F.; Kalz, H. *Angew. Chem., Int. Ed. Engl.* **1987**, *26*, 371.

(2) Schaefer, D. *Science* **1989**, *243*, 1023.

(3) Segal, D. *Chem. Br.* **1989**, *2*, 151.

(4) Schmidt, W.; Interrante, L.; Doremus, R.; Trout, T.; Marchetti, P.; Maciel, G. *Chem. Mater.* **1991**, *3*, 257.

(5) Laine, R.; Babonneau, F. *Chem. Mater.* **1993**, *5*, 260.

(6) Peuckert, M.; Vaahs, T.; Brück, M. *Adv. Mater.* **1990**, *9*, 398.

(7) Paciorek, K.; Masuda, S.; Kratzer, R.; Schmidt, W. *Chem. Mater.* **1991**, *3*, 88.

(8) Partridge, G. *Adv. Mater.* **1993**, *5*, 747.

(9) Rye, R.; Tallant, D.; Borek, T.; Lindquist, D.; Paine, R. *Chem. Mater.* **1991**, *3*, 286.

(10) Seyferth, D.; Lang, H.; Sobon, C.; Borm, J.; Tracy, H. J.; Bryson, N. J. *Inorg. Organomet. Polym.* **1992**, *2*, 59.

(11) Seyferth, D.; Czubarow, P. *Chem. Mater.* **1994**, *6*, 10.

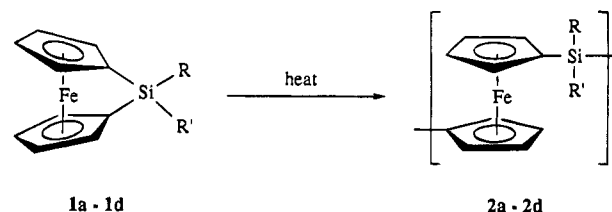
MC/MSi/SiC or SiC/MN composites.<sup>12–14</sup> Polymers containing skeletal transition-metal atoms might also be expected to be useful pyrolytic precursors to metal-containing ceramics. However, this approach is virtually unexplored due, in part, to the limited number of readily accessible and well-characterized materials available.

We have previously shown that poly(ferrocenylsilanes) are accessible via the ring-opening polymerization (ROP) of strained, silicon-bridged [1]ferrocenophanes.<sup>15</sup> Subsequent work has shown that the ROP of [n]-metallocenophanes is quite general and provides a versatile route to a variety of metallocene-based polymers containing silicon or other elements in the polymer backbone.<sup>16–20</sup> We also reported that symmetrically substituted poly(ferrocenyldimethylsilane) and poly(ferrocenyldiphenylsilane) are thermally stable to ca. 350 °C but at more elevated temperatures yield magnetic iron silicon carbide ceramics together with novel, molecular depolymerization byproducts.<sup>17</sup> In this paper we report full details of our work designed to assess the potential of poly(ferrocenylsilanes) to function as pre-ceramic polymers. Specifically, we report on the pyrolysis of a series of poly(ferrocenylsilanes) and the characterization and properties of the resulting solid-state and molecular products.

## Results and Discussion

High molecular weight poly(ferrocenylsilanes) are readily accessible via thermal, anionic, or transition-metal-catalyzed ROP of silicon-bridged [1]ferrocenophanes.<sup>15,16,21</sup> The latter species are synthesized from dilithioferrocene-tmeda (tmeda = tetramethylethylenediamine) and organodichlorosilanes. As a wide variety of these species are available from the silicone industry, poly(ferrocenylsilanes) with a range of different substituents can be prepared. A crucial issue with respect to the use of these materials as preceramic polymers is the ceramic yield. The versatility of poly(ferrocenylsilanes) is potentially advantageous in this respect as the introduction of side groups which promote cross-linking rather than depolymerization should be possible. In addition, given reasonable ceramic yields, side-group versatility may allow tuning of ceramic composition. In this paper we describe our studies of the pyrolysis of

the poly(ferrocenylsilanes) **2a–d** derived from the thermal ROP of **1a–d**.<sup>18,19</sup>



	R	R'
<b>1a, 2a</b>	Me	Me
<b>1b, 2b</b>	Ph	Ph
<b>1c, 2c</b>	Me	H
<b>1d, 2d</b>	Me	Vinyl

**Synthesis of Poly(ferrocenylsilanes) 2a–d.** The poly(ferrocenylsilanes) **2a–d** were prepared via the thermal ROP of the [1]ferrocenophanes **1a–d**.<sup>18,19</sup> The red-orange, moisture-sensitive, crystalline monomers **1a–d** were purified by sublimation or recrystallization from THF/hexanes in 60–70% yield. Polymers **2a–d** were obtained from **1a–d** by heating these species at 120–150 °C for ca. 30 min. During this time the tube contents became molten, increasingly more viscous, and then immobile. Purification was achieved by dissolution in THF followed by precipitation into hexanes except in the case of polymer **2b**, which is insoluble in common polar organic solvents unless the molecular weight is moderate or low ( $M_w < \text{ca. } 5 \times 10^4$ ). The molecular weights of **2a**, **2c**, and **2d** were in the range  $M_w = 1.6 \times 10^5$ – $8.6 \times 10^5$  and  $M_n = 7.7 \times 10^4$ – $4.3 \times 10^5$ . Yields of the poly(ferrocenylsilanes) were ca. 80–90%.

**Studies of the Pyrolysis of the Poly(ferrocenylsilane) 2a under Dinitrogen.** (i) *Thermogravimetric Analysis.* Thermogravimetric analysis (TGA) studies of the polymer **2a** under  $\text{N}_2$  using a heating rate of 10 °C/min showed that this material was stable to weight loss until ca. 350 °C (Figure 1). Above this temperature two distinct weight-loss processes were detected. An initial weight loss of approximately 50% occurred between 350 and 525 °C with a subsequent weight loss of approximately 14% being observed between 575 and 650 °C. Further thermolysis up to 1000 °C led to very little change in mass. The final char yield for this polymer was 36% (Table 1). To analyze the products formed at elevated temperatures, pyrolysis studies were conducted in a tube furnace.

(ii) *Pyrolysis Studies in a Tube Furnace.* Samples of the polymer **2a** were heated at either 400, 600, 800, or 1000 °C for 4 h under a slow flow of dinitrogen with this temperature being attained in 1 h. Pyrolyses yielded black and lustrous materials that were readily attracted to a bar magnet and an orange sublimate which condensed on the cooler parts of the tube. In cases where the polymer was ground and compressed or in the form of a film prior to heating, some shape retention was observed. When multiple pyrolyses were carried out simultaneously, ceramic yields were always higher at the effluent end of the tube. This can be rationalized by a shift in the depolymerization/cross-linking equilibrium due to the presence of additional depolymerization products formed from polymer decom-

(12) Corriu, R. J. P.; Gerbier, P.; Guerin, C.; Henner, B.; Jean, A.; Mutin, P. H. *Organometallics* **1992**, *11*, 2507.

(13) Corriu, R. J. P.; Douglas, W.; Layher, E.; Shankar, R. J. *Inorg. Organomet. Polym.* **1993**, *3*, 129.

(14) Corriu, R. J. P.; Gerbier, P.; Guerin, C.; Henner, B. *Angew. Chem., Int. Ed. Engl.* **1992**, *31*, 1195.

(15) Foucher, D. A.; Tang, B. Z.; Manners, I. *J. Am. Chem. Soc.* **1992**, *114*, 6246.

(16) Manners, I. *Adv. Organomet. Chem.* **1995**, *37*, 131 and references therein.

(17) Tang, B.; Petersen, R.; Foucher, D.; Lough, A.; Coombs, N.; Sodhi, R.; Manners, I. *J. Chem. Soc., Chem. Commun.* **1993**, 523.

(18) Foucher, D. A.; Ziembinski, R.; Tang, B. Z.; Macdonald, P. M.; Massey, J.; Jaeger, C. R.; Vancso, G. J.; Manners, I. *Macromolecules* **1993**, *26*, 2878.

(19) Foucher, D.; Ziembinski, R.; Petersen, R.; Pudelski, J.; Edwards, M.; Ni, Y.; Massey, J.; Jaeger, R. C.; Vancso, J. G.; Manners, I. *Macromolecules* **1994**, *27*, 3992.

(20) For the work of other groups on poly(ferrocenylsilanes) and related polymers, see: (a) Rosenberg, H. US Patent 3,426,053, 1969. (b) Tanaka, M.; Hayashi, T. *Bull. Chem. Soc. Jpn.* **1993**, *66*, 334. (c) Nguyen, M. T.; Diaz, A. F.; Dement'ev, V. V.; Pannell, K. H. *Chem. Mater.* **1993**, *5*, 1389. (d) Hmyene, M.; Yasser, A.; Escorne, M.; Percheron-Guegan, A.; Garnier, F. *Adv. Mater.* **1994**, *6*, 564.

(21) (a) Rulkens, R.; Ni, Y.; Manners, I. *J. Am. Chem. Soc.* **1994**, *116*, 12121. (b) Ni, Y.; Rulkens, R.; Pudelski, J. K.; Manners, I. *Makromol. Chem. Rapid Commun.* **1995**, *16*, 637.

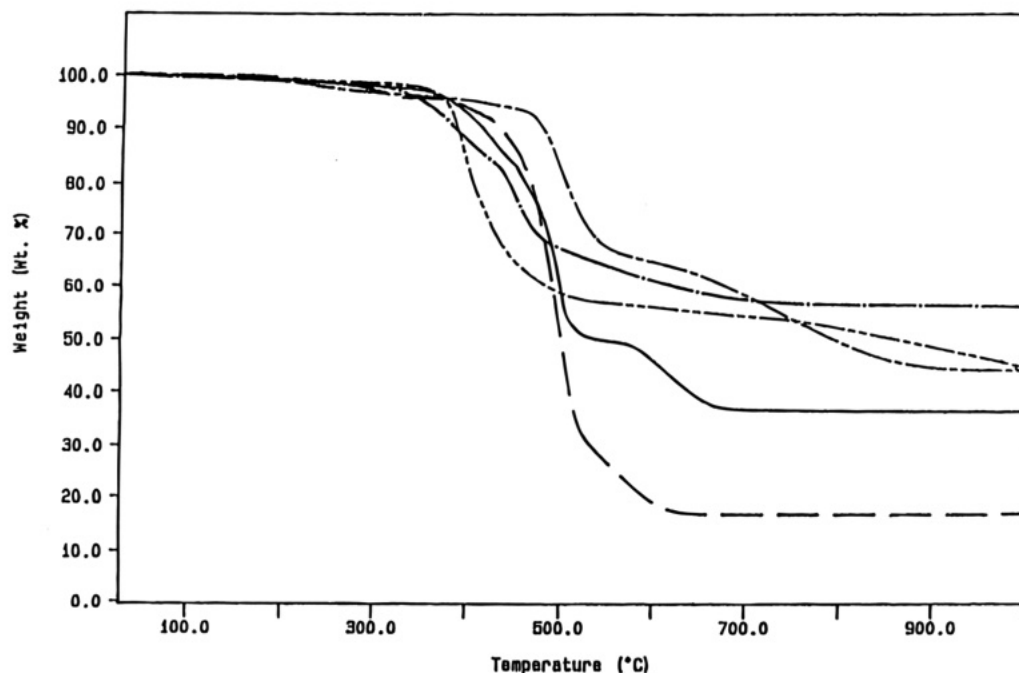


**Figure 1.** TGA thermogram of the polymers **2a–d** and the polymer blend **2c/d** carried out under a flow of dinitrogen at a heating rate of 10 °C/min. **2a** (—), **2b** (---), **2c** (- · - · -), **2d** (- - -), **2c/d** (- · - · -).

**Table 1.** TGA Yields at 600 and 1000 °C for the Ceramics **3a–e** Formed under Dinitrogen

ceramic	percent yield at 600 °C	percent yield at 1000 °C
<b>3a</b>	47	36
<b>3b</b>	18	17
<b>3c</b>	58	45
<b>3d</b>	66	44
<b>3e</b>	62	56

position reactions. High dinitrogen flow rates resulted in lower ceramic yields and an increase in the quantity of volatile byproducts produced. Moreover, polymer pyrolysis at 600 °C for 4 h under a dynamic vacuum of ca.  $10^{-5}$  mmHg gave a ceramic yield of 11% which was considerably lower than under dinitrogen (31%). These results are also consistent with a competition between cross-linking and depolymerization, leading to either ceramic formation or volatilization during thermolysis.

**Characterization of the Ceramic Product 3a, Derived from the Pyrolysis of 2a under Dinitrogen at 600 and 1000 °C.** The solid-state pyrolysis product, **3a**, formed during thermolysis of **2a** at 600 and 1000 °C under dinitrogen, was investigated using high-resolution scanning electron microscopy (SEM) with energy-dispersive X-ray microanalysis (EDX) and back-scattered electron imaging (BEI), C and H elemental analysis, X-ray photoelectron spectroscopy (XPS), X-ray powder diffraction (XRD), magnetization measurements, and Mössbauer spectroscopy.

The ceramic **3a** produced at 600 °C was qualitatively similar to the ceramic **3a** formed at 1000 °C. Analysis by high-resolution SEM to 2500× magnification in both cases showed a smooth topology, with no signs of crystallinity such as grain boundaries (Figure 2). Furthermore, no segregation of the elements was observed by BEI which indicated that the ceramic produced at both temperatures was homogeneous, at least down to a length scale of ca. 30 nm. EDX studies carried out using a sample of the polymer **2a** as a compositional standard, showed that the ceramic **3a** formed at 600 °C contained approximately 30% iron, 17% silicon and 50% carbon whereas the analogous ceramic formed at

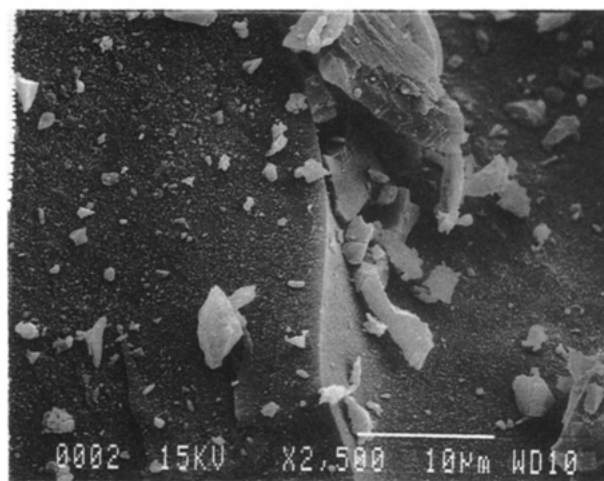


**Figure 2.** SEM of the ceramic **3a** formed at 600 °C under an atmosphere of dinitrogen shown at 2500× magnification.

1000 °C contained 11% iron, 30% silicon, and 58% carbon. Elemental analysis indicated that only a trace of hydrogen was present (0.4% for the ceramic formed at 600 °C, 0.3% for that prepared at 1000 °C). For both ceramics, EDX detected small quantities of oxygen (ca. less than 5%). However, XPS studies on **3a** formed at 600 °C showed the ceramic surface to be composed primarily of carbon (79.6%) with significant quantities of oxygen (14.5%) also present. The source of this oxygen is not clear; however, these results suggest it may arise from exposure of the ceramic to air after pyrolysis as the surface is much more oxygen-rich than the bulk. A powder X-ray diffractogram of **3a** at 600 °C showed a small, broad peak at a  $d$  spacing of 2.02(9) Å, which was sharper and much more intense in the diffractogram of the ceramic formed at 1000 °C. This peak and the peaks located at 1.43(3) and 1.17(3) Å  $d$  spacings are attributed to  $\alpha$ -Fe (Figure 3).<sup>22</sup> BEI carried out on the ceramic **3a** formed at 1000 °C showed no localized iron sites, which suggests that the  $\alpha$ -Fe sites are smaller than ca. 30 nm. The crystallite size was estimated from the powder XRD pattern of the ceramic

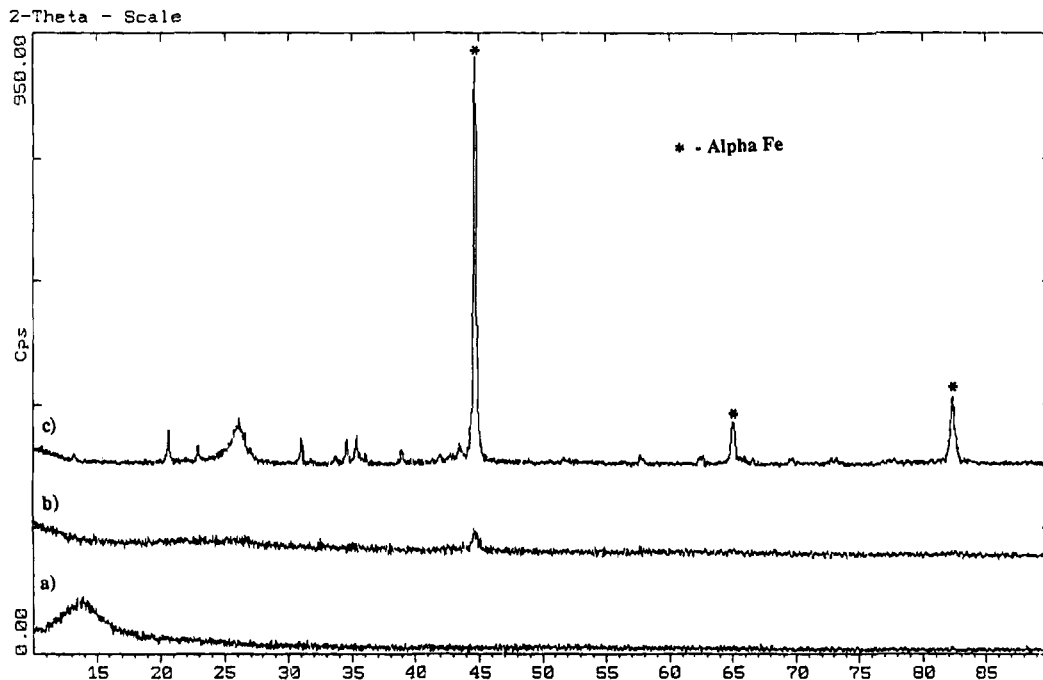


**Figure 3.** Powder X-ray diffractogram of (a) the polymer **2a**, (b) the ceramic **3a** produced at 600 °C, and (c) the ceramic **3a** produced at 1000 °C under atmospheres of N<sub>2</sub>. \* =  $\alpha$ -Fe.

formed at 1000 °C. The full width at half-height of the main peak suggests a crystallite size of ca. 20 nm according to the Scherrer equation:

$$L_{hkl} = [(2 \cos \theta) \delta\theta / \lambda]^{-1}$$

where  $L_{hkl}$  is the average length dimension of the crystallite in the  $[hkl]$  direction,  $\delta\theta$  the full width at half-height (in radians),  $\lambda$  the wavelength of the X-ray radiation used, and  $\theta$  the Bragg angle for this reflection ( $2\theta = 44.65^\circ$  in this case).<sup>23</sup>

The ceramic samples of **3a** were readily attracted to a bar magnet which suggested ferromagnetic behavior. This was confirmed by a study of the magnetization as a function of the applied field at 25 °C which exhibited a hysteresis cycle typical for a soft magnetic material (Figure 4). For the ceramic formed at 600 °C the observed coercive field,  $H_c$ , was 40 G, the remnant magnetization,  $M_r$ , was 0.013  $\mu_B/\text{Fe}$ , and the saturation magnetization,  $M_s$ , was ca. 0.17  $\mu_B/\text{Fe}$ . For the ceramic formed at 1000 °C, the corresponding values were  $H_c = 171$  G,  $M_r = 0.103 \mu_B/\text{Fe}$ , and  $M_s = \text{ca. } 1.65 \mu_B/\text{Fe}$ .

Mössbauer spectra obtained at 25 °C of the polymer **2a** and the ceramics **3a** formed at 600 and 1000 °C are shown in Figure 5. The spectrum of the polymer **2a** shows a quadrupolar doublet with a quadrupolar splitting (QS) of 2.34 mm/s consistent with an Fe<sup>2+</sup> site. The ceramics display more complex spectra consistent with magnetic iron sites arising from the lifting of the degeneracy of the  $I = \pm 1/2$  and  $\pm 3/2$  states. Interestingly, the ceramic **3a** synthesized at 600 °C displayed a six-line Mössbauer spectrum arising from magnetic iron sites on which was superimposed a quadrupolar doublet. The latter is consistent with the presence of iron in a chemically different, nonmagnetic environment as has

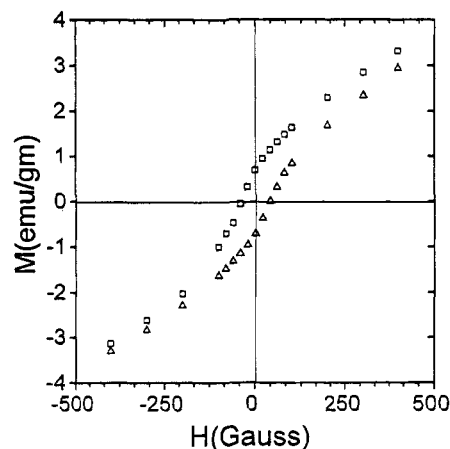


**Figure 4.** Field-dependant magnetization (at 25 °C) of the ceramic **3a** formed at 600 °C under an atmosphere of dinitrogen.

been found in certain iron-carbon steel formulations or, alternatively, the presence of superparamagnetic iron where the very small magnetic domains can rapidly reorient.<sup>24</sup> By contrast, only a characteristic six-line Mössbauer spectrum was observed for the ceramic **3a** formed at 1000 °C.

**Characterization of the Volatile Byproducts Derived from the Pyrolysis of 2a under Dinitrogen at 600 °C.** The orange sublimation products formed above ca. 350 °C during the pyrolysis of **2a** were separated on an alumina column using dichloromethane and hexane elutants. These products were characterized using <sup>1</sup>H, <sup>13</sup>C NMR, mass spectrometry, and in one case by single-crystal X-ray diffraction and cyclic voltammetry.

The first iron-containing species which eluted from the column formed orange, needlelike crystals upon

(22) International Center for Diffraction Database, *Powder Diffraction File, Inorganic Phases*; Joint Committee on Powder Diffraction Standards: Pennsylvania, 1989; Alphabetical Listing (Hanawalt Method); p 299.

(23) Klug, H. P.; Alexander, L. E. *Powder X-ray Diffraction Techniques*; J. Wiley & Sons: New York, 1974; p 541.

(24) (a) Gruverman, I. J. *Mössbauer Effective Methodology*; Plenum Press: New York, 1967; Vol. 3, pp 37-65. (b) Gruverman, I. J. *Mössbauer Effective Methodology*; Plenum Press: New York, 1967; Vol. 3, pp 103-122.

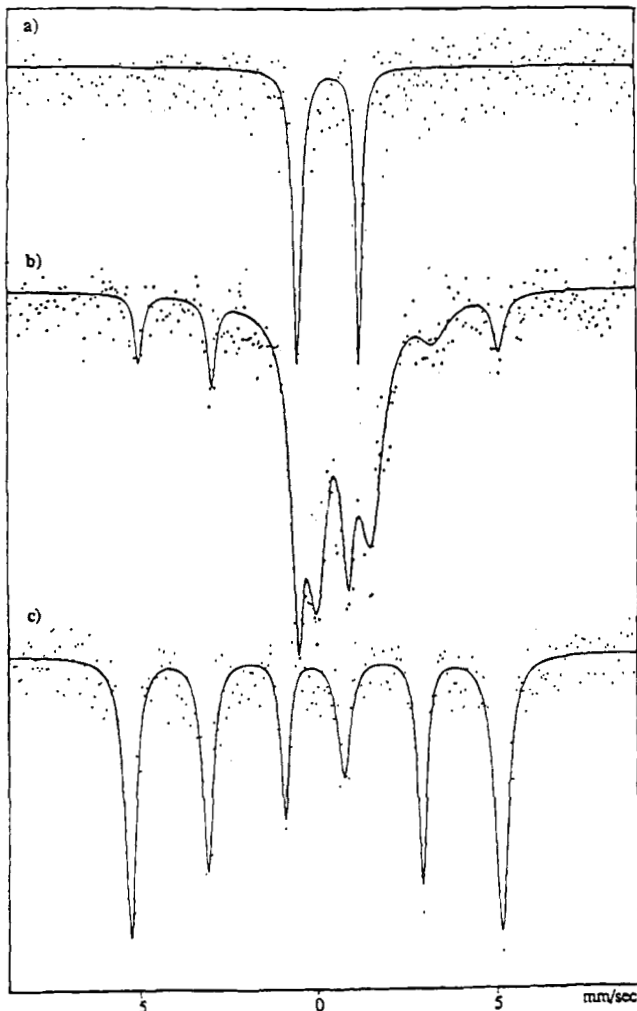
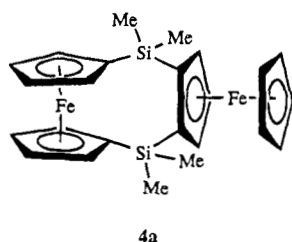


**Figure 5.** Mössbauer spectra obtained at 25 °C of the (a) the polymer **2a**, (b) the ceramic **3a** formed at 600 °C, and (c) the ceramic **3a** formed at 1000 °C under atmospheres of dinitrogen.

evaporation in air. This was shown to be ferrocene by  $^1\text{H}$  and  $^{13}\text{C}$  NMR. The second product isolated yielded crystals that were analyzed initially by mass spectrometry and by  $^1\text{H}$  NMR (in  $\text{CDCl}_3$ ). Mass spectrometry gave a parent peak located at  $m/z$  484 which corresponded to a dimer of the [1]ferrocenophane monomer **1a**. However, the  $^1\text{H}$  NMR spectrum of this species was complex and showed that the cyclopentadienyl ligands were not equivalent. Broad multiplets of  $\delta = 4.20\text{--}4.41$  and  $\delta = 4.00\text{--}4.18$  ppm were detected, which were assigned to substituted cyclopentadienyl groups. In addition a singlet resonance at  $\delta = 4.19$  ppm was detected consistent with the presence of an unsubstituted  $\eta\text{-C}_5\text{H}_5$  group. Single-crystal X-ray diffraction (see below) identified this product as the unusual unsymmetrical dimer  $\text{Fe}(\eta\text{-C}_5\text{H}_4)_2(\mu\text{-SiMe}_2)_2(\eta\text{-C}_5\text{H}_3)\text{Fe}(\eta\text{-C}_5\text{H}_5)$ , **4a**.



The other products that eluted from the column could not be identified by  $^1\text{H}$  NMR and mass spectrometry

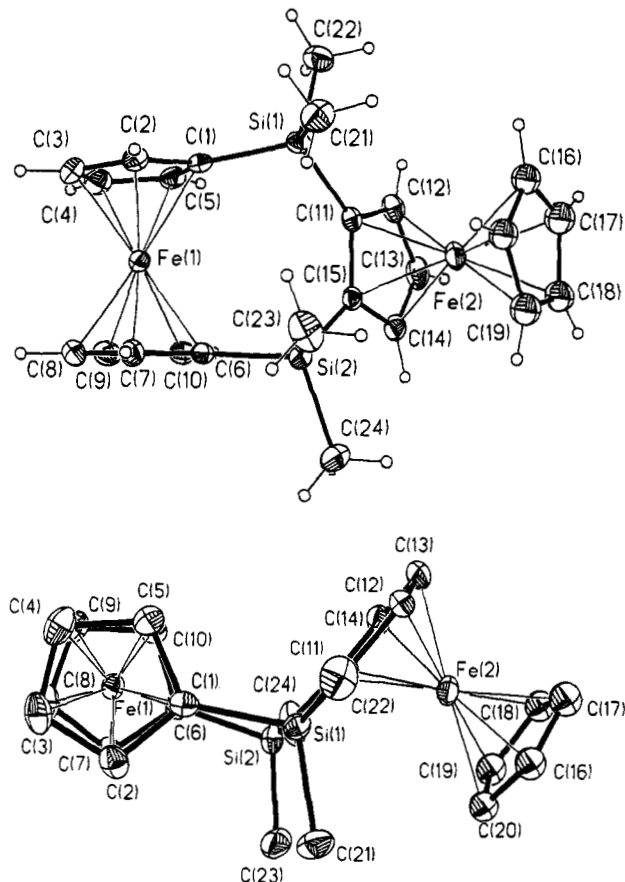


**Figure 6.** (a) Side-on view of the molecular structure of **4a**. (b) Alternative view of the molecular structure of **4a**.

due to the complexity of the spectra observed.

**X-ray Structure of 4a.** Single crystals of **4a**, suitable for an X-ray diffraction study, were grown from hexanes via solvent evaporation. Two views of the molecular structure of **4a** are shown in Figure 6. A summary of cell constants and data collection parameters are included in Table 2. Final fractional atomic co-ordinates are given in Table 3.

The X-ray crystal structure of **4a** consists of molecules with two ferrocene moieties oriented perpendicular to one another, joined through two bridging  $\text{SiMe}_2$  units. One ferrocene unit can be regarded as a [4]ferrocenophane and one cyclopentadienyl ligand of the other is bound via adjacent carbons to two silicon atoms of the bridge. The Cp ligands of the 1,1'-disubstituted ferrocene fragment are staggered by an angle of  $5.7(4)^\circ$ . Interestingly, the mean planes of these ligands are not parallel but are tilted away from the bridge by an angle of  $5.7(2)^\circ$ . The resultant displacement of the iron atom from the line joining the centroids of the Cp ligands is very small ( $0.057(3)$  Å) and the angles between the planes of the Cp ligands and the ipso C–Si bonds are  $6.4(2)$  and  $2.3(2)^\circ$  for C(1) and C(6), respectively. The angle between the planes of the Cp rings in the 1,2-disubstituted ferrocene fragment is smaller ( $3.5(2)^\circ$ ). The Cp–Si–Cp bond angles in **4a** are  $108.8(1)^\circ$  and  $106.8(1)^\circ$  and are characteristic of  $\text{sp}^3$ -hybridized silicon. The distance between the two iron atoms Fe(1) and Fe(2) is  $5.820(5)$  Å.

**Cyclic Voltammetry of 4a.** A cyclic voltammogram of **4a** in  $\text{CH}_2\text{Cl}_2$  at a scan rate of  $250 \text{ mV s}^{-1}$  is shown in Figure 7. Two reversible one-electron oxidation waves were detected due to the interaction between the

**Table 2. Summary of Crystal Data and Intensity Collection Parameters for 4a**

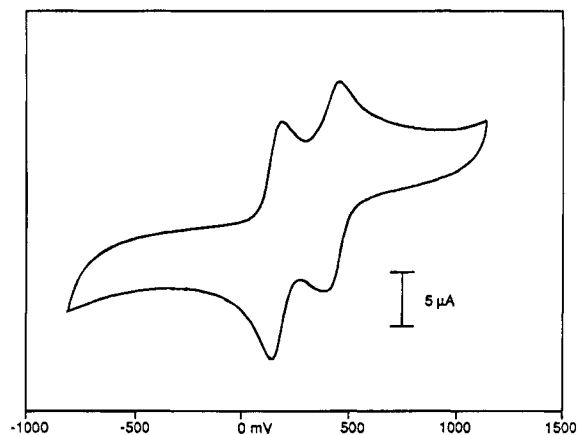
4a	
empirical formula	C <sub>24</sub> H <sub>28</sub> Fe <sub>2</sub> Si <sub>2</sub>
M <sub>r</sub>	484.3
cryst class	monoclinic
space group	P2 <sub>1</sub> /n
a, Å	9.3842(8)
b, Å	15.455(2)
c, Å	15.6630(12)
α, deg	
β, deg	91.092(6)
γ, deg	
V, Å <sup>3</sup>	2271.2(11)
Z	4
D <sub>calc</sub> , g cm <sup>-3</sup>	1.416
μ(Mo Kα), cm <sup>-1</sup>	0.14
F(000)	1008
ω-scan width, deg	0.6 + 0.35 tan θ
range θ collected, deg	1.0 to 45.0
total no. of rflns	3099
no. of unique rflns	2998
R <sub>int</sub>	1.80
no. of obsd data used [I > 3σ(I)]	2580
weighting g	0.0001
R	0.028
R <sub>w</sub>	0.031
GOF	2.02
(Δσ) <sub>max</sub> in last cycle	0.05
no. of params refined	281
Δρ(max) in final ΔF map, e Å <sup>-3</sup>	0.22

**Table 3. Non-Hydrogen Atom Fractional Coordinates (×10<sup>4</sup>) and Equivalent Isotropic Displacement Coefficients (Å<sup>2</sup> × 10<sup>3</sup>) for 4a, with Estimated Standard Deviations in Parentheses<sup>a</sup>**

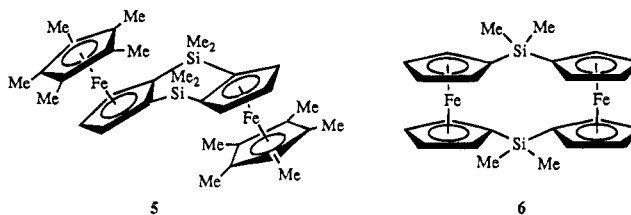
	x	y	z	U(eq)
Fe(1)	2650(1)	4067(1)	5749(1)	33(1)
Fe(2)	7686(1)	1937(1)	6344(1)	44(1)
Si(1)	4848(1)	3046(1)	7374(1)	35(1)
Si(2)	4576(1)	2235(1)	5052(1)	39(1)
C(1)	3490(3)	3821(2)	6964(2)	34(1)
C(2)	1971(3)	3754(2)	6941(2)	47(1)
C(3)	1388(3)	4560(2)	6669(2)	57(1)
C(4)	2518(4)	5124(2)	6511(2)	57(1)
C(6)	3405(3)	3182(2)	4871(2)	34(1)
C(5)	3804(3)	4673(2)	6689(2)	42(1)
C(7)	1876(3)	3216(2)	4855(2)	44(1)
C(8)	1437(3)	4071(2)	4657(2)	53(1)
C(9)	2661(3)	4576(2)	4552(2)	53(1)
C(10)	3868(3)	4042(2)	4689(2)	42(1)
C(11)	6246(3)	2918(2)	6562(2)	32(1)
C(12)	7681(3)	3209(2)	6698(2)	46(1)
C(13)	8452(3)	3103(2)	5946(2)	55(1)
C(14)	7528(3)	2745(2)	5324(2)	47(1)
C(15)	6142(3)	2622(2)	5684(2)	33(1)
C(17)	9243(4)	1286(3)	6995(2)	70(1)
C(18)	9186	1021	6128	64(1)
C(19)	7808	677	5954	65(1)
C(20)	7013	730	6714	67(1)
C(16)	7900	1106	7358	69(1)
C(17A)	8566(4)	1238(3)	7325(2)	70(1)
C(18A)	9438	1197	6595	63(1)
C(19A)	8623	821	5919	65(1)
C(20A)	7248	629	6230	69(1)
C(16A)	7212	887	7100	66(1)
C(21)	3982(3)	2035(2)	7731(2)	61(1)
C(22)	5698(4)	3550(2)	8337(2)	64(1)
C(23)	3501(4)	1349(2)	5522(2)	73(1)
C(24)	5223(4)	1847(3)	4001(2)	83(1)

<sup>a</sup> Equivalent isotropic U defined as one-third of the trace of the orthogonalized U<sub>ij</sub> tensor.

iron atoms in the two ferrocenyl moieties. Oxidation of the first iron at a potential of 0.06 V was found to increase the oxidation potential of the remaining iron atom to 0.32 V relative to the ferrocene/ferrocenium couple. The redox coupling for **4a**, ΔE<sub>1/2</sub>, is 0.26 V. By

**Figure 7.** Cyclic voltammogram of **4a** in CH<sub>2</sub>Cl<sub>2</sub> at a scan rate of 250 mV/s at 25 °C. The x-axis scale is referenced to the ferrocene/ferrocenium ion couple at E = 0.0 mV.

comparison, bis(ferrocenyl)dimethylsilane, which has two ferrocene units bridged by a single SiMe<sub>2</sub> unit, and the dimer **5** which possesses two ferrocenyl moieties



linked by two adjacent SiMe<sub>2</sub> units, show two reversible one-electron oxidation waves with ΔE<sub>1/2</sub> values of 0.15 and 0.27 V, respectively.<sup>25–27</sup> Interestingly, the symmetrical dimer, **6**, which we and others have recently synthesized and characterized, possesses two parallel ferrocene moieties linked through two SiMe<sub>2</sub> units.<sup>28</sup> This species has an Fe–Fe distance of 5.171(9) Å, which is significantly shorter than that in **4a** but possesses a very similar redox coupling (ΔE<sub>1/2</sub> = 0.25 V). These results suggest that the interaction between the iron atoms is more dependent on the type of bridge, which involves two silicon atoms in each case, than on the spatial proximity of the iron centers.

**Studies of the Pyrolysis of the Poly(ferrocenylsilane) 2a in Air at 600 °C.** The pyrolysis of **2a** in air was carried out in a tube furnace at 600 °C for 4 h. The resulting ceramic was an orange-red solid and was less readily attracted to a bar magnet than the corresponding ceramic **3a** formed by pyrolysis under dinitrogen. The yields obtained from the pyrolysis under air (46%) were slightly higher than the corresponding pyrolysis of **2a** under dinitrogen (31%).

SEM-EDX and BEI studies carried out on a ground sample of the ceramic product (see Figure 8) showed it to be homogeneous down to a length scale of ca. 30 nm. EDX showed the ceramic to contain iron, silicon, carbon,

(25) Bocarsly, A. B.; Walton, E. G.; Bradley, M. G.; Wrighton, M. S. *J. Electroanal. Chem. Interfacial Electrochem.* **1979**, *100*, 283.

(26) Kreiszi, J.; Kirss, R. U.; Reiff, M. W. *Inorg. Chem.* **1994**, *33*, 1562.

(27) The interaction between two ferrocenyl units has been shown to decrease with increasing length of an oligosilane spacer: Dementev, V. V.; Cervantes-Lee, F.; Parkanyi, L.; Sharma, H.; Pannell, K. H.; Nguyen, M. T.; Diaz, A. *Organometallics* **1993**, *12*, 1983.

(28) (a) Zechel, D.; Foucher, D. F.; Pudelski, J. K.; Yap, G. P. A.; Rheingold, A. L.; Manners, I. *J. Chem. Soc., Dalton Trans.* **1995**, 1893. (b) Park, J.; Seo, Y.; Cho, S.; Whang, D.; Kim, K.; Chang, T. *J. Organomet. Chem.* **1995**, *489*, 23.

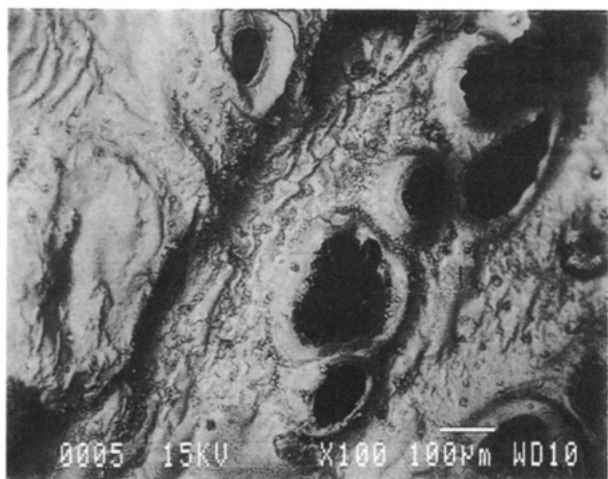


**Figure 8.** SEM of the ceramic **3a** formed at 600 °C via pyrolysis in air.

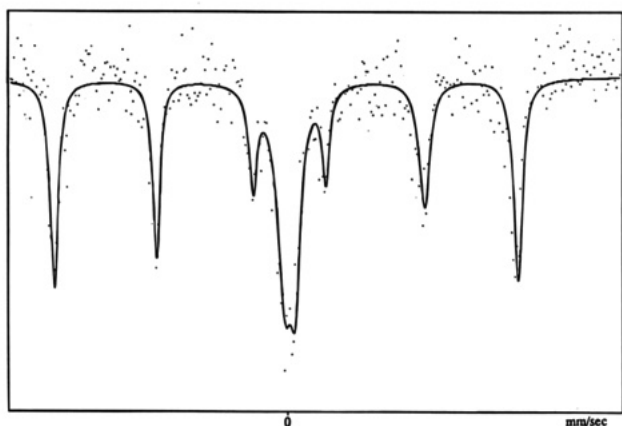


**Figure 9.** Mössbauer spectrum of the ceramic **3a** formed at 600 °C via pyrolysis in air.

and oxygen in a ratio of 57:6:13:24% and XPS indicated an oxygen and carbon rich surface composition (O 45.4%, C 38.7%). The Mössbauer spectrum of this ceramic (Figure 9) was qualitatively similar to that detected for the ceramic **3a** formed at 600 °C under dinitrogen (see Figure 5) and displayed a six-line pattern characteristic of an internal magnetic field and a central peak characteristic of nonmagnetic iron with a very small, virtually unresolved, quadrupolar splitting ( $<0.25$  mm/s). A magnetization study of this material also yielded a hysteresis cycle with  $H_c = 66$  G,  $M_r = 0.001 \mu_B/Fe$ , and  $M_s = 0.01 \mu_B/Fe$ . In contrast to the pyrolysis of **2a** under dinitrogen, ceramic formation in air was not accompanied by the formation of isolable volatile byproducts.

**Studies of the Pyrolysis of the Poly(ferrocenylsilanes) 2b–d and a Blend of 2c and 2d.** (i) *Thermogravimetric Analysis.* The TGA traces for the polymers **2b–d** in  $N_2$  show very little weight loss when heated to 350 °C (Figure 1). However, further heating revealed a dramatic weight loss resulting in ceramic yields of 18% (for **2b**) to 66% (**2d**) at 600 °C. Further heating to 1000 °C resulted in similar or slightly decreased ceramic yields of which the highest was that for **2c** (45%). Because of the possibility of enhancing thermally induced cross-linking via hydrosilylation the pyrolysis of a 1:1 molar ratio of the polymers **2c** and **2d** was also investigated. The blend gave a ceramic yield of 62% at 600 °C and the highest yield at 1000 °C (56%, see Table 1).

(ii) *Pyrolysis Studies in a Tube Furnace at 600 °C under Dinitrogen.* Pyrolysis of the polymers **2b–d** and the polymer blend **2c/2d** were carried out under  $N_2$  with a 1 h heating ramp from room temperature to 600 °C and subsequent thermolysis for 4 h at this temperature. Ceramics were obtained as black, lustrous materials in yields of ca. 25%, 64%, and 65% from the polymers **2b**, **2c**, and **2d**, respectively. As found for the pyrolysis of **2a**, concurrent with the onset temperature for weight loss by TGA the formation of a yellow-orange sublimate was observed on the cooler section of the quartz tube downstream from the polymer sample. This was also attributed to the loss of molecular fragments during the decomposition of the polymers **2b–d** and the conversion to ceramic. The relatively low ceramic yield for **2b** suggests that depolymerization is favored by the presence of bulky phenyl groups. The higher ceramic yields for **2c** and **2d** might be expected based on the favorable preceramic properties of organosilicon polymers with Si–H groups and the propensity of the vinyl substituent to undergo thermally induced cross-linking reactions.<sup>5</sup> These two factors can be attributed to the overall higher char yield for the blend of these two polymers.

**Characterization of the Ceramic and Depolymerization Products Formed via the Pyrolysis of the Poly(ferrocenylsilanes) 2b–d and the Blend of 2c and 2d at 600 °C under Dinitrogen.** The ceramics **3b** and **3e** derived from **2b** and the polymer blend **2c/2d** at 600 °C were characterized as representative examples in a manner similar to **3a** formed at the same temperature. In both cases an amorphous, ferromagnetic iron silicon carbide composition was indicated. For **3b**, SEM-EDX indicated that the bulk ceramic had a higher carbon content than **3a** with a composition of Fe 21%, Si 10%, C 69% consistent with the higher carbon content of the starting polymer **2b**. XPS showed the surface to contain 85.7% carbon with an appreciable quantity of oxygen (6.3%). The ceramic **3e**, derived from the blend at 600 °C, displayed a rougher topology by SEM than the ceramics **3a** and **3b** and was found by EDX to contain iron, silicon, carbon and oxygen ratio of 19:24:50:7%. Magnetization measurements for **3b** and **3e** yielded quantitatively similar results to those for **3a**. The observed coercive field for **3b**,  $H_c$ , was 83 G, the remnant magnetization,  $M_r$ , was  $0.019 \mu_B/Fe$ , and the saturation magnetization,  $M_s$ , was ca.  $0.09 \mu_B/Fe$ . For the ceramic **3e**, the  $H_c$  was 177 G,  $M_r$  was  $0.064 \mu_B/Fe$  and  $M_s$  was  $0.42 \mu_B/Fe$ . The Mössbauer spectrum for **3b** was qualitatively similar to that for **3a** at 600 °C and was indicative of the presence of both magnetic and nonmagnetic iron sites.

The sublimate formed during the pyrolysis of **2b** was collected using dichloromethane and was separated on an alumina column using hexanes/dichloromethane as elutents. A number of products were obtained. The first band afforded orange needlelike crystals that were analyzed by  $^1H$  NMR and determined to be ferrocene. The second product was also eluted using hexanes and was also obtained as light orange needlelike crystals. However, a  $^1H$  and  $^{13}C$  NMR spectrum of this species suggested their identity to be triphenylsilylferrocene,  $Fe(\eta-C_5H_5)(\eta-C_5H_4SiPh_3)$ . Analysis by mass spectrometry supported this assignment and showed the presence of a molecular ion peak at  $m/e$  444 together with peaks corresponding to logical fragmentation products. The formation of this interesting product suggests that

the phenyl groups are undergoing thermally induced migration reactions during the pyrolysis process. Subsequent products eluted from the column could not be isolated pure or identified.

The depolymerization products formed during the pyrolysis of the polymer **2c** were analyzed by  $^1\text{H}$  NMR and were found to consist primarily of ferrocene. The volatile byproducts produced during the pyrolysis of **2d** and the blend **2c/2d** were not successfully separated nor characterized.

### Summary

Poly(ferrocenylsilanes) yield black, lustrous, ferromagnetic iron-silicon-carbon-containing ceramics when heated at or above 400 °C. TGA analysis showed that the "functionalized" polymers **2c** (with Si-H groups) and **2d** (with vinyl groups) give the highest ceramic yields at 600 °C under dinitrogen (ca. 60–65%) and a 1:1 polymer blend of **2c** and **2d** was found to give the highest ceramic yield at 1000 °C (56%). The results are consistent with competition between cross-linking to give a 3-dimensional ultrastructure and the formation of molecular depolymerization products. We have successfully characterized an unusual example of the latter; the dimer **4a** formed during the pyrolysis of **2a**. Further work will involve the design of poly(ferrocenylsilanes) with substituents which promote cross-linking to further increase ceramic yields to the stage where good shape retention can be anticipated during the pyrolysis of polymer fibers, films, or coatings.

### Experimental Section

**General Comments.** The silicon-bridged [1]ferrocenophanes were synthesized under an atmosphere of prepurified dinitrogen using solvents which were dried by standard techniques and distilled under dinitrogen. Solvents required for the purification and isolation of the poly(ferrocenylsilanes) and other materials were used as received.

The 200 or 400 MHz  $^1\text{H}$  NMR spectra and 50.3 or 100.5 MHz  $^{13}\text{C}$  NMR spectra were recorded either on a Varian Gemini 200 or a Varian XL 400 spectrometer, respectively. All solution NMR spectra were referenced internally to TMS. Mass spectra were obtained with the use of a VG 70-250S mass spectrometer operating in Electron Impact (EI) mode. Polymer molecular weights were estimated by gel permeation chromatography (GPC) in THF using a Waters Associates liquid chromatograph equipped with a 510 HPLC pump, U6K injector, ultrastragel columns with a pore size between  $10^3$  and  $10^5$  Å, and a Waters 410 differential refractometer which were calibrated with polystyrene standards. A flow rate of 1.0 mL/min was used, and samples were dissolved in a solution of 0.1% tetra-*n*-butylammonium bromide in THF. In the case of **2b**, the molecular weight could not be obtained as the polymer is insoluble.

A Perkin-Elmer TGA-7 thermal gravimetric analyzer equipped with a TAC-7 instrument controller was used to study the polymer thermal stability. Thermograms were calibrated with the magnetic transitions of Nicoseal and Perkalloxy and were obtained at a heating rate of 10 °C/min under dinitrogen. Pyrolyses were carried out in air or under an atmosphere of prepurified nitrogen, using a 36 in. long, three-zone Lindberg Pyrolysis Oven Model No. 55035 with a 1 $\frac{5}{8}$  in. internal diameter and Thermcraft control system Model 3D1-50-115 (UP27) with type K thermocouples and independent oven temperature control. A program was created that ramped to the desired temperature over 1 h. Polymer samples were loaded in quartz boats, 2 in.  $\times$  1/2 in. and inserted into quartz pyrolysis tubes, 36 in. long with a 1 in. external diameter, equipped with quartz liners, 32 in. long with a 3/4 in. external diameter.

Scanning electron micrographs were obtained on a Hitachi Model S-570 field emission scanning electron microscope using an accelerating voltage of 20 keV. Energy-dispersive X-ray (EDX) microanalyses were performed on uncoated samples tilted 15° toward the detector at a distance of 15 mm. Samples of the polymeric ceramic precursors were used as compositional standards for the Fe, Si, and C calibrations. Errors in the compositional values obtained are considered to be  $\pm 5\%$  for Fe and Si and  $\pm 10\%$  for C. XPS data was collected on a Leybold MAX 200 instrument. Values obtained are based on the integration of the following peaks Fe (2p $_{3/2}$ , 708.1 eV), Si (2p, 102.4 eV), C (1s, 284.6 eV), O (1s, 533.2 eV). Mössbauer spectra were obtained using a 5 mCi  $^{57}\text{Co}$   $\gamma$ -ray source in a Rh matrix on a Ranger Scientific Inc. VT-1200 instrument equipped with a MS-1200 digital channel analyzer. Data were collected as long as required to attain a suitable fit and interpreted using a C program for a PC and fit to standard independent Lorentzian line shapes for sinusoidal baselines.<sup>29</sup> Data were in the -15.8 to +15.8 mm/s range and referenced to Fe foil. X-ray powder diffraction data were obtained using a Siemens D500 diffractometer employing Ni-filtered Cu K $\alpha$  ( $\lambda = 1.54178$  Å) radiation. Samples were scanned at step widths of 0.02° with 1.0 s per step in the Bragg angle range of 5–90°. Samples were prepared by spreading finely ground ceramic samples on grooved glass slides. Magnetization curves were measured at room temperature using a Quantum Design SQUID magnetometer. Elemental Analyses were carried out by Quantitative Technologies Incorporated in Whitehouse, NJ.

Cyclic voltammetry of **4a** was carried out using a PAR Model 273 potentiostat with a Pt working electrode, a W secondary electrode, and an Ag wire reference electrode in a Luggin capillary. The solution of **4a** was  $4 \times 10^{-4}$  M in  $\text{CH}_2\text{Cl}_2$  with 0.1 M  $[\text{Bu}_4\text{N}][\text{PF}_6]$  as a supporting electrolyte.

**Synthesis of the Poly(ferrocenylsilanes) 2a–d.** The monomers **1a–d** were synthesized according to published literature procedures using dilithioferrocene complexed to tmeda and the corresponding distilled organodichlorosilane.<sup>18,19</sup> Purification was carried out by high-vacuum sublimation or recrystallization from THF/hexanes. Polymer synthesis was carried out according to previously published results by heating prepurified silicon bridged [1]ferrocenophanes in a sealed and evacuated Pyrex tube at temperatures ranging from 120 to 150 °C for ca. 30 min. Polymer purification was achieved by dissolution in THF and precipitation into hexanes in the case of **2a**, **2c**, and **2d** and by washing with hexanes in the case of **2b**. Characterization data for **2a–d** has been previously reported.<sup>18,19</sup> Molecular weights data were obtained via GPC:

$$\mathbf{2a}: M_w = 4.9 \times 10^5, M_n = 3.2 \times 10^5, \text{polydispersity } (M_w/M_n) = 1.5$$

$$\mathbf{2c}: M_w = 8.6 \times 10^5, M_n = 4.3 \times 10^5, \text{polydispersity } (M_w/M_n) = 2.0$$

$$\mathbf{2d}: M_w = 1.6 \times 10^5, M_n = 7.7 \times 10^4, \text{polydispersity } (M_w/M_n) = 2.1$$

**Synthesis of the 1:1 Blend of Poly(ferrocenylsilanes) 2c and 2d.** Samples of **2c** (0.20 g, 0.86 mmol) and **2d** (0.22 g, 0.86 mmol) were dissolved separately in ca. 5 mL of distilled THF, and the solutions combined together under an atmosphere of dinitrogen. The volume of the resulting solution was then reduced by half, and the resulting solution precipitated into a solution of dry hexanes. The resulting polymer was dark yellow (0.38 g, 90%).  $^1\text{H}$  NMR ( $\text{C}_6\text{D}_6$ ) showed the blend to be a 1:1 mixture of **2c** and **2d**.

**Pyrolysis of Powdered Samples of the Poly(ferrocenylsilanes) 2a–d and the 1:1 Blend of 2c/2d under Dinitrogen.** Powdered samples of **2a** were pyrolyzed at 400, 600, 800, and 1000 °C. The pyrolyses of samples of **2b–d** and **2c/2d** were carried out at 600 °C. Pyrolysis of **2a–d** and **2c/d**

(29) Chile, J.; Holmes, A. J. Personal Computer Program, University of Toronto, Toronto, 1990.



yielded the ceramics **3a–e**, respectively, together with an orange-yellow sublimate consisting of molecular depolymerization products. The procedures used were similar and the pyrolysis of **2a** at 600 °C is used as a typical example.

A sample of **2a** (0.35 g, 1.5 mmol) was lightly packed into a quartz boat, and inserted into a pyrolysis tube. The tube was purged with a steady flow of dinitrogen for approximately one minute before it was reduced to a rate of ca. 0.5 mL/s. A program was created that heated the system from 25 to 600 °C over 1 h and maintained a constant temperature of 600 °C for a further 4 h. After approximately 30 min from the initiation of the heating program, which corresponded to a temperature of ca. 350 °C, an orange-yellow sublimate condensed on the cooler parts of the pyrolysis tube. When the program was complete, the furnace was allowed to cool to room temperature. A black, lustrous ceramic product was formed, yield 0.11 g (31%). This product was found to be readily attracted to a bar magnet. The orange-yellow sublimate was collected by rinsing the tube with hexanes and was also analyzed.

The yields of the ceramic **3a** were found to be as follows: 400 °C, 37%; 600 °C, 31%; 800 °C, 31%; 1000 °C, 16%. The molecular byproducts formed during the thermolysis of **2a** were isolated in the following yields: 400 °C, 10%; 600 °C, 20%; 800 °C, 20%; 1000 °C, 20% relative to **2a**. The yields of **3b**, **3c**, **3d**, and **3e** at 600 °C were 25%, 64%, 65%, and 59%, respectively. Molecular byproduct yields were as follows: **3b**, 47%; **3c**, 19%; **3d**, 27%; **3e**, 13%.

**3a** (derived from **2a** at 600 °C): EDX: Fe 30, Si 17, C 50, O 3%. XPS: Fe 0.8, Si 5.1, C 79.6, O 14.5%. Elemental analysis: 46.4% C, 0.4% H. XRD: Featureless except for a low-intensity sharp line at a *d* spacing of 2.03 Å. Magnetization measurements:  $H_c = 40$  G,  $M_r = 0.013 \mu_B/\text{Fe}$ ,  $M_s = \text{ca. } 0.17 \mu_B/\text{Fe}$ . Mössbauer spectrum: sextuplet IS = 0.01, MHS =  $2.1 \text{ mm s}^{-1}$ , doublet IS = 0.30, QS =  $0.86 \text{ mm s}^{-1}$ .

**3a** (derived from **2a** at 1000 °C): EDX: Fe 11, Si 30, C 58, O 1%. XPS: Fe 1.0, Si 10.4, C 70.0, O 18.6%. Elemental analysis: 51.2% C, 0.3% H. XRD: peaks attributed to  $\alpha$ -Fe had *d* spacings of 2.02(6), 1.43(3), and 1.17(3) Å. Other peaks were observed at 4.29(7), 3.86(9), 3.39(6), 2.87(8), 2.65(6), 2.59(3), 2.53(6), 2.31(3), 2.15(1), 2.07(8), 1.59(7), and 1.34(8) Å *d* spacings.

Magnetization measurements:  $H_c = 171$  G,  $M_r = 0.103 \mu_B/\text{Fe}$ ,  $M_s = \text{ca. } 1.65 \mu_B/\text{Fe}$ . Mössbauer spectrum: sextuplet, IS =  $0.03 \text{ mm s}^{-1}$ , MHS =  $1.65 \text{ mm s}^{-1}$ .

**3b** (derived from **2b** at 600 °C): EDX Fe 21, Si 10, C 69%. XPS Fe 2.0, Si 6.0, C 85.6, O 6.3%. XRD: Featureless except for low-intensity sharp lines at *d* spacings of 2.38(5), 2.10(7), 2.07(3), 2.02(3), 1.97(8), and 1.84(7) Å. Magnetization measurements:  $H_c = 83$  G,  $M_r = 0.019 \mu_B/\text{Fe}$ ,  $M_s = 0.09 \mu_B/\text{Fe}$ . Mössbauer spectrum: sextuplet IS = 0.93, MHS =  $1.45 \text{ mm s}^{-1}$ , doublet IS = 0.80, QS =  $1.93 \text{ mm s}^{-1}$ .

**3e** (derived from a 1:1 molar ratio blend of **2c** and **2d** at 600 °C): EDX Fe 19, Si 24, C 50, O 7%. XRD: Featureless except for peaks attributed to  $\alpha$ -Fe with *d* spacings of 2.02(9), 1.43(4), and 1.17(1) Å. Magnetization measurements:  $H_c = 177$  G,  $M_r = 0.064 \mu_B/\text{Fe}$ ,  $M_s = \text{ca. } 0.42 \mu_B/\text{Fe}$ .

**Pyrolysis of 2a under Vacuum.** A powdered sample of **2a** (0.063 g, 0.26 mmol) was packed into a quartz boat, loaded into the tube furnace, and placed under a dynamic vacuum of ca.  $10^{-5}$  mmHg. The sample was then ramped to 600 °C over 1 h and heating was continued at this temperature a further 4 h. After cooling, the black lustrous material formed was removed and weighed (0.007 g, 11%). The sublimate was collected by rinsing with hexanes and THF (0.047 g, 75%).

**Pyrolysis of Thin Films of 2a under Dinitrogen.** Films of **2a** were cast on a Teflon plate from THF via evaporation. The resulting orange film (0.017 g, 0.070 mmol) was pyrolyzed

in a quartz boat at 400 °C for 2 h. The resulting ceramic film weighed 0.008 g (ca. 50%).

**Characterization of the Volatile Sublimate Formed during the Pyrolysis of Powdered Samples of 2a.** The sublimate that condensed on the cooler part of the tube during the pyrolysis of **2a** at 600 °C was dissolved in hexanes and was then chromatographed on alumina. The three bands obtained were reduced in volume on a rotary evaporator and allowed to evaporate in air. The resulting products were characterized. Band A was found to consist of ferrocene (0.09 g, 32%) which was identified by  $^1\text{H}$  and  $^{13}\text{C}$  NMR. Light orange needlelike crystals.  $^1\text{H}$  NMR ( $\text{C}_6\text{D}_6$ )  $\delta = 4.18$  (s,  $\eta\text{-C}_5\text{H}_5$ ) ppm;  $^{13}\text{C}$  NMR ( $\text{C}_6\text{D}_6$ )  $\delta = 72.0$  ( $\eta\text{-C}_5\text{H}_5$ ) ppm.

Band B yielded pale orange needlelike crystals (0.02 g, 3%) which were analyzed by  $^1\text{H}$  NMR, mass spectrometry, and single-crystal X-ray diffraction and found to be the unsymmetrical dimer **4a**.  $^1\text{H}$  NMR ( $\text{C}_6\text{D}_6$ )  $\delta = 4.41\text{--}4.20$  (m, 8H, Cp), 4.19 (s, 5H,  $\eta\text{-C}_5\text{H}_5$ ), 4.18–4.00 (m, 3H, Cp), 0.55–0.15 (m, 12H,  $\text{CH}_3$ ) ppm. MS (EI, 70eV) *m/z* (%) 484 (100,  $\text{M}^+$ ), 469 (22,  $\text{M}^+ - \text{CH}_3$ ), 419 (14,  $\text{M}^+ - \text{Cp}$ ). Band C yielded a mixture of pale orange powders and oils (0.12 g) which could not be separated or identified.

**Pyrolysis of 2a in Air.** A quartz boat was packed with purified polymer **2a** (0.140 g, 0.58 mmol), loaded in a quartz tube and placed in the tube furnace. The polymer heated in 1 h to 600 °C and that temperature maintained for 4 h. The ceramic material formed was an orange-red material (0.064 g, 46%). No volatile sublimate was recovered.

**3a** (derived from **2a** at 600 °C under an air atmosphere): EDX: Fe 57, Si 6, C 13, O 24%. XPS: Fe 1.4, Si 14.5, C 38.7, O 45.4%. XRD: Featureless except for sharp lines at *d* spacings of 3.68(3), 2.69(9), 2.51(5), 2.07(4), 1.69(5), and 1.47(2) Å. Mössbauer spectrum: sextuplet IS = 0.38, MHS =  $3.4 \text{ mm s}^{-1}$ , doublet IS = 0.35, QS =  $0.25 \text{ mm s}^{-1}$ ; Magnetization measurements:  $H_c = 66$  G,  $M_r = 0.001 \mu_B/\text{Fe}$ ,  $M_s = 0.01 \mu_B/\text{Fe}$ .

**Characterization of the Volatile Sublimate Formed during the Pyrolysis of 2b.** The sublimate formed during the pyrolysis of **2b** was analyzed in a way similar to that from **2a** and gave three bands after column chromatography.

Band A was found to consist of ferrocene (0.027 g, 25%) which was identified as in the case for the pyrolysis of **2a**.

Band B yielded pale orange needlelike crystals which were identified as triphenylsilylferrocene (0.026 g, 9%).

$^1\text{H}$  NMR ( $\text{CDCl}_3$ )  $\delta = 7.37$  (br, m, 6H, Ph), 7.36 (br, m, 9H, Ph), 4.44 (m, 2H, Cp), 4.33 (m, 2H, Cp), 3.88 (s, 5H, Cp).

MS (EI, 70 eV) *m/z* (%) 445 (50,  $\text{M}^+ + 1$ ), 444 (100,  $\text{M}^+$ ), 379 (27,  $\text{M}^+ - \text{Cp}$ ), 369 (15,  $\text{M}^+ - \text{Ph}$ ). The third band comprised products that could not be separated nor identified (0.217 g).

**Acknowledgment.** This work was funded by the Institute for Chemical Science and Technology (ICST) and the Natural Science and Engineering Research Council of Canada (NSERC) Industrially Oriented Research (IOR) Program. We thank C. V. Stager for use of the SQUID magnetometer and Prof. G. A. Ozin and Prof. R. Morris for the use of their Mössbauer and electrochemical equipment, respectively. I.M. is also grateful to the Alfred P. Sloan Foundation for a Research Fellowship (1994–96).

**Supporting Information Available:** Crystal data for **4a** (13 pages); observed and calculated structure factors (7 pages). Ordering information is given on any current masthead page.

CM9500768